Available online at www.sciencedirect.com
ScienceDirect
Journal of Sound and Vibration 317 (2008) 250–264
JOURNAL OF SOUND AND VIBRATION
www.elsevier.com/locate/jsvi

Wave propagation in non-homogeneous magneto-electro-elastic plates

Wu Bin[a], Yu Jiangong[a,b,*], He Cunfu[a]

[a]College of Mechanical Engineering and Applied Electronic Technology, Beijing University of Technology, Ping Le Yuan 100#, Chaoyang District, Beijing 100022, PR China
[b]School of Mechanical and Power Engineering, Henan Polytechnic University, Jiaozuo 454003, PR China

Received 11 July 2007; received in revised form 23 February 2008; accepted 4 March 2008
Handling Editor: L.G. Tham

Abstract

A dynamic solution is presented for the propagation of harmonic waves in imhomogeneous (functionally graded) magneto-electro-elastic plates composed of piezoelectric $BaTiO_3$ and magnetostrictive $CoFe_2O_4$. The materials properties are assumed to vary in the direction of the thickness according to a known variation law. The Legendre orthogonal polynomial series expansion approach is employed to determine the wave propagating characteristics in the plates. The dispersion curves of the imhomogeneous piezoelectric–piezomagnetic plate and the corresponding non-piezoelectric, non-piezomagnetic plates are calculated to show the influences of the piezoelectricity and piezomagnetism on the dispersion curves. They are compared with the dispersion curves of the plates with the different magnetic constants to illustrate the influential factors of the piezoelectric and piezomagnetic effect for the wave propagation in a magneto-electro-elastic plate. Electric potential and magnetic potential distributions at different wavenumbers are also obtained to illustrate the different influences of the piezoelectricity and piezomagnetism.

1. Introduction

Over the past few years, the mechanics of the piezoelectric–piezomagnetic composites has received considerable research effort with their increasing usage in various applications, including sensors and actuators [1,2]. These composites possess particular product properties, i.e. the magneto–electric coupling effect, which are not demonstrated with their individual components.

The structural analysis of magneto-electro-elastic plates and shells has received much attention. Using a propagator matrix method, Pan [3] derived an exact three-dimensional solution for a simply supported multilayered orthotropic magneto-electro-elastic plate. Pan and Heyliger [4] investigated the free vibration of piezoelectric–magnetostrictive plate. They found that some natural frequencies of a piezoelectric–magnetostrictive plate were identical to the ones of the corresponding elastic plate. Chen et al. [5] showed theoretically

*Corresponding author at: College of Mechanical Engineering and Applied Electronic Technology, Beijing University of Technology, Ping Le Yuan 100#, Chaoyang District, Beijing 100022, PR China. Tel.: +86 10 67391720 11.
E-mail address: yu@emails.bjut.edu.cn (Y. Jiangong).

0022-460X/$ - see front matter
doi:10.1016/j.jsv.2008.03.008

that there actually exists a class of vibration, of which the frequencies depend on the elastic property only. Wang and Shen [6] derived the general solution of three-dimensional problems in transversely isotropic magneto-electro-elastic media and obtained the fundamental solution for dislocation and Green's functions in half-space. Wang and Shen [7] also studied the two-dimensional problem of inclusions of arbitrary shape in magneto-electro-elastic composites. Hou and Leung [8] obtained the analytical solution for the axisymmetric plane strain magneto-electro-elastic dynamics of hollow cylinders. Chen et al. [9] derived the General solution for transversely isotropic magneto-electro-thermo-elasticity. Hou et al. [10] studied the transient responses of a special non-homogeneous magneto-electro-elastic hollow cylinder for axisymmetric plane strain problem.

Wave propagating in magneto-electro-elastic media has also attracted the attention of researchers. Chen and Shen [11] obtained effective wave velocity and attenuation factor when axial shear magneto-electro-elastic waves propagate in piezoelectric–piezomagnetic composites. Using the 'rod model', Wei and Su [12] studied the axisymmetric flexural wave in piezoelectric-piezomannelic cylinders. Chen and Chen [13] investigated the Love wave behavior in magneto-electro-elastic multilayered structures by the propagation matrix method. Using the propagator matrix and state-vector (or state space) approaches, an analytical treatment is presented for the propagation of harmonic waves in magneto-electro-elastic multilayered plates by Chen et al. [14].

In this paper, the propagation of harmonic waves in imhomogeneous magneto-electro-elastic plates composed of piezoelectric and magnetostrictive materials is investigated by the Legendre orthogonal polynomial series expansion approach, which was developed by Lefebvre for modeling free-ultrasonic waves in multilayered plates [15] and functionally graded piezoelectric plates [16]. The dispersion curves for the imhomogeneous magneto-electro-elastic plates and the corresponding non-piezoelectric and non-piezo-magnetic plates are calculated to show the influences of the piezoelectricity and piezomagnetism. Electric potential and magnetic potential distributions at different wavenumbers are obtained to illustrate the different influences of the piezoelectricity and piezomagnetism. In this paper, the open circuit is assumed.

2. Mathematics and formulation of the problem

Consider an anisotropic, magneto-electro-elastic FGM plate, which is infinite horizontally with a thickness h. We place the horizontal (x,y)-plane of a cartesian coordinate system on the bottom surface and let the plate be in the positive z-region.

For a linear, anisotropic and magneto-electro-elastic solid, the coupled constitutive equation can be written in the following form:

$$\begin{Bmatrix} T_{xx} \\ T_{yy} \\ T_{zz} \\ T_{yz} \\ T_{xz} \\ T_{xy} \end{Bmatrix} = \begin{bmatrix} C_{11} & C_{12} & C_{13} & C_{14} & C_{15} & C_{16} \\ & C_{22} & C_{23} & C_{24} & C_{25} & C_{26} \\ & & C_{33} & C_{34} & C_{35} & C_{36} \\ & & & C_{44} & C_{45} & C_{46} \\ & \text{symmetry} & & & C_{55} & C_{56} \\ & & & & & C_{66} \end{bmatrix} \begin{Bmatrix} \varepsilon_{xx} \\ \varepsilon_{yy} \\ \varepsilon_{zz} \\ 2\varepsilon_{yz} \\ 2\varepsilon_{xz} \\ 2\varepsilon_{xy} \end{Bmatrix} - \begin{bmatrix} e_{11} & e_{21} & e_{31} \\ e_{12} & e_{22} & e_{32} \\ e_{13} & e_{23} & e_{33} \\ e_{14} & e_{24} & e_{34} \\ e_{15} & e_{25} & e_{35} \\ e_{16} & e_{26} & e_{36} \end{bmatrix} \begin{Bmatrix} E_x \\ E_y \\ E_z \end{Bmatrix}$$

$$- \begin{bmatrix} q_{11} & q_{21} & q_{31} \\ q_{12} & q_{22} & q_{32} \\ q_{13} & q_{23} & q_{33} \\ q_{14} & q_{24} & q_{34} \\ q_{15} & q_{25} & q_{35} \\ q_{16} & q_{26} & q_{36} \end{bmatrix} \begin{Bmatrix} H_x \\ H_y \\ H_z \end{Bmatrix}, \tag{1a}$$

$$\begin{Bmatrix} D_x \\ D_y \\ D_z \end{Bmatrix} = \begin{bmatrix} e_{11} & e_{12} & e_{13} & e_{14} & e_{15} & e_{16} \\ e_{21} & e_{22} & e_{23} & e_{24} & e_{25} & e_{26} \\ e_{31} & e_{32} & e_{33} & e_{34} & e_{35} & e_{36} \end{bmatrix} \begin{Bmatrix} \varepsilon_{xx} \\ \varepsilon_{yy} \\ \varepsilon_{zz} \\ 2\varepsilon_{yz} \\ 2\varepsilon_{xz} \\ 2\varepsilon_{xy} \end{Bmatrix} + \begin{bmatrix} \in_{11} & \in_{12} & \in_{13} \\ & \in_{22} & \in_{23} \\ \text{symmetry} & & \in_{33} \end{bmatrix} \begin{Bmatrix} E_x \\ E_y \\ E_z \end{Bmatrix}$$

$$+ \begin{bmatrix} g_{11} & g_{12} & \varepsilon_{13} \\ & \varepsilon_{22} & \varepsilon_{23} \\ \text{symmetry} & & \varepsilon_{33} \end{bmatrix} \begin{Bmatrix} H_x \\ H_y \\ H_z \end{Bmatrix}, \tag{1b}$$

$$\begin{Bmatrix} B_x \\ B_y \\ B_z \end{Bmatrix} = \begin{bmatrix} q_{11} & q_{12} & q_{13} & e_{14} & q_{15} & q_{16} \\ q_{21} & q_{22} & q_{23} & q_{24} & q_{25} & q_{26} \\ q_{31} & q_{32} & q_{33} & q_{34} & q_{35} & q_{36} \end{bmatrix} \begin{Bmatrix} \varepsilon_{xx} \\ \varepsilon_{yy} \\ \varepsilon_{zz} \\ 2\varepsilon_{yz} \\ 2\varepsilon_{xz} \\ 2\varepsilon_{xy} \end{Bmatrix} + \begin{bmatrix} g_{11} & g_{12} & g_{13} \\ & g_{22} & g_{23} \\ \text{symmetry} & & g_{33} \end{bmatrix} \begin{Bmatrix} E_x \\ E_y \\ E_z \end{Bmatrix}$$

$$+ \begin{bmatrix} \mu_{11} & \mu_{12} & \mu_{13} \\ & \mu_{22} & \mu_{23} \\ \text{symmetry} & & \mu_{33} \end{bmatrix} \begin{Bmatrix} H_x \\ H_y \\ H_z \end{Bmatrix}, \tag{1c}$$

where T_{ij}, D_i and B_i are the stress, electric displacement and magnetic induction, respectively; ε_{ij}, E_i and H_i are the strain, electric field and magnetic field, respectively; C_{ij}, e_{ij} and q_{ij} are the elastic, piezoelectric and piezomagnetic coefficients, respectively; $\in_{ij}$, g_{ij}, and μ_{ij} are the dielectric, magneto–electric, and magnetic permeability coefficients, respectively.

The relationship between the general strain and general displacement can be expressed as

$$\begin{aligned} &\varepsilon_{xx} = \frac{\partial u_x}{\partial x}, \quad \varepsilon_{yy} = \frac{\partial u_y}{\partial y}, \quad \varepsilon_{zz} = \frac{\partial u_z}{\partial z}, \quad \varepsilon_{yz} = \frac{1}{2}\left(\frac{\partial u_y}{\partial z} + \frac{\partial u_z}{\partial y}\right), \quad \varepsilon_{xz} = \frac{1}{2}\left(\frac{\partial u_x}{\partial z} + \frac{\partial u_z}{\partial x}\right), \\ &\varepsilon_{xy} = \frac{1}{2}\left(\frac{\partial u_x}{\partial y} + \frac{\partial u_y}{\partial x}\right), \quad E_x = -\frac{\partial \Phi}{\partial x}, \quad E_y = -\frac{\partial \Phi}{\partial y}, \quad E_z = -\frac{\partial \Phi}{\partial z}, \\ &H_x = -\frac{\partial \Psi}{\partial x}, \quad H_y = -\frac{\partial \Psi}{\partial y}, \quad H_z = -\frac{\partial \Psi}{\partial z}, \end{aligned} \tag{2}$$

where u_i is the elastic displacement, and Φ and Ψ are the electric potential and magnetic potential.

For the wave propagation considered in this paper, the body forces, electric charge and current density are assumed to be zero. Thus, the dynamic equation for the magneto-electro-elastic plate is governed by

$$\frac{\partial T_{xx}}{\partial x} + \frac{\partial T_{xy}}{\partial y} + \frac{\partial T_{xz}}{\partial z} = \rho \frac{\partial^2 u_x}{\partial t^2},$$

$$\frac{\partial T_{xy}}{\partial x} + \frac{\partial T_{yy}}{\partial y} + \frac{\partial T_{yz}}{\partial z} = \rho \frac{\partial^2 u_y}{\partial t^2},$$

$$\frac{\partial T_{xz}}{\partial x}+\frac{\partial T_{yz}}{\partial y}+\frac{\partial T_{zz}}{\partial z}=\rho\frac{\partial^2 u_z}{\partial t^2},$$
$$\frac{\partial D_x}{\partial x}+\frac{\partial D_y}{\partial y}+\frac{\partial D_z}{\partial z}=0$$
$$\frac{\partial B_x}{\partial x}+\frac{\partial B_y}{\partial y}+\frac{\partial B_z}{\partial z}=0 \tag{3}$$

with ρ being the density of the material.

Because the material properties vary in the thickness direction, the elastic constants of the medium are the function of z

$$C(z)=C^{(0)}+C^{(1)}\left(\frac{z}{h}\right)^1+C^{(2)}\left(\frac{z}{h}\right)^2+\cdots+C^{(L)}\left(\frac{z}{h}\right)^L.$$

With implicit summation over repeated indices, $C(z)$ can be written compactly as

$$C(z)=C^{(l)}z^l \quad l=0,1,2,\ldots,L.$$

And other material constants can be treated in the same way,

$$\rho(z)=\rho^{(l)}\left(\frac{z}{h}\right)^l,\quad e_{ij}(z)=e_{ij}^{(l)}\left(\frac{z}{h}\right)^l,\quad \varepsilon_{ij}(z)=\varepsilon_{ij}^{(l)}\left(\frac{z}{h}\right)^l,\quad q_{ij}(z)=q_{ij}^{(l)}\left(\frac{z}{h}\right)^l,$$
$$g_{ij}(z)=g_{ij}^{(l)}\left(\frac{z}{h}\right)^l,\quad \mu_{ij}(z)=\mu_{ij}^{(l)}\left(\frac{z}{h}\right)^l,\quad l=0,1,2,\ldots,L. \tag{4}$$

Considering the boundary of the material for an open circuit surface, the position dependence of the elastic, dielectric, piezoelectric constants and mass density is given by

$$\bar{C}(z)=C(z)\pi(h),\quad \bar{\rho}(z)=\rho(z)\pi(h),\quad \bar{e}(z)=e(z)\pi(h),\quad \bar{\varepsilon}(z)=\varepsilon(z)\pi(h),$$
$$\bar{q}(z)=q(z)\pi(h),\quad \bar{g}(z)=g(z)\pi(h),\quad \bar{\mu}(z)=\mu(z)\pi(h), \tag{5}$$

where $\pi(h)$ is the rectangular window function defined by

$$\pi(h)=\begin{cases}1, & 0\leqslant z\leqslant h,\\ 0, & \text{elsewhere.}\end{cases}$$

Given Eq. (5), the material constants vanish outside the material. We thus describe the vacuum outside the material as a medium with zero acoustic impedance and zero electric displacement, which ensures that $T_{zz}=T_{xz}=T_{yz}=0$ and $D_z=0$, $B_z=0$ when $z=0$, $z=h$.

For a free harmonic wave being propagated in the x direction in a plate, we assume the displacement components, electric potential and magnetic potential to be of the form

$$u_x(x,y,z,t)=\exp(\mathrm{i}kx-\mathrm{i}\omega t)U(z), \tag{6a}$$

$$u_y(x,y,z,t)=\exp(\mathrm{i}kx-\mathrm{i}\omega t)V(z), \tag{6b}$$

$$u_z(x,y,z,t)=\exp(\mathrm{i}kx-\mathrm{i}\omega t)W(z), \tag{6c}$$

$$\Phi(x,y,z,t)=\exp(\mathrm{i}kx-\mathrm{i}\omega t)X(z), \tag{6d}$$

$$\Psi(x,y,z,t)=\exp(\mathrm{i}kx-\mathrm{i}\omega t)Y(z). \tag{6e}$$

$U(z)$, $V(z)$ and $W(z)$ represent the amplitude of vibration in the x, y and z directions, respectively, and $X(z)$ and $Y(z)$ represent the amplitudes of electric potential and magnetic potential. k is the magnitude of the wave vector in the propagation direction, and ω is the angular frequency.

Substituting Eqs. (1), (2), (4)–(6) into Eq. (3), the governing differential equations in terms of displacement components, electric potential and magnetic potential can be obtained:

$$\begin{aligned}&\left(\frac{z}{h}\right)^l\Big[C_{55}^{(l)}U''+C_{45}^{(l)}V''+C_{35}^{(l)}W''+e_{35}^{(l)}X''+q_{35}^{(l)}Y''+2\mathrm{i}kC_{15}^{(l)}U'+\mathrm{i}k\left(C_{14}^{(l)}+C_{56}^{(l)}\right)V'\\&+lz^{-1}\left(C_{55}^{(l)}+C_{45}^{(l)}V'+C_{35}^{(l)}W'+e_{35}^{(l)}X'+q_{35}^{(l)}Y'\right)+\mathrm{i}k\left(C_{13}^{(l)}+C_{55}^{(l)}\right)W'\\&+\mathrm{i}k\left(e_{15}^{(l)}+e_{31}^{(l)}\right)X'+\mathrm{i}k\left(q_{15}^{(l)}+q_{31}^{(l)}\right)Y'-k^2\left(C_{11}^{(l)}U+C_{16}^{(l)}V+C_{15}^{(l)}W+e_{11}^{(l)}X+q_{11}^{(l)}Y\right)\\&+l\mathrm{i}kz^{-1}\left(C_{15}^{(l)}U+C_{56}^{(l)}V+C_{55}^{(l)}W+e_{15}^{(l)}X+q_{15}^{(l)}Y\right)\Big]\pi(z)\\&+(\delta(z-0)-\delta(z-h))\left(\frac{z}{h}\right)^l\left(C_{55}^{(l)}U'+C_{45}^{(l)}V'+C_{35}^{(l)}W'+e_{35}^{(l)}X'+q_{35}^{(l)}Y'+\mathrm{i}kC_{15}^{(l)}U\right.\\&\left.+\mathrm{i}kC_{56}^{(l)}V+\mathrm{i}kC_{55}^{(l)}W+\mathrm{i}ke_{15}^{(l)}X+ikq_{15}^{(l)}Y\right)=-\frac{\rho^{(l)}z^l\omega^2}{h^l}U\pi(z),\end{aligned}\tag{7a}$$

$$\begin{aligned}&\left(\frac{z}{h}\right)^l\Big[C_{45}^{(l)}U''+C_{44}^{(l)}V''+C_{34}^{(l)}W''+e_{34}^{(l)}X''+q_{34}^{(l)}Y''+\mathrm{i}k\left(C_{14}^{(l)}+C_{56}^{(l)}\right)U'+2\mathrm{i}kC_{46}^{(l)}V'\\&+\mathrm{i}k\left(C_{36}^{(l)}+C_{45}^{(l)}\right)W'+lz^{-1}\left(C_{45}^{(l)}U'+C_{44}^{(l)}V'+C_{34}^{(l)}W'+e_{34}^{(l)}X'+q_{34}^{(l)}Y'\right)\\&+\mathrm{i}k\left(e_{14}^{(l)}+e_{36}^{(l)}\right)X'+\mathrm{i}k\left(q_{14}^{(l)}+q_{36}^{(l)}\right)Y'-k^2\left(C_{16}^{(l)}U+C_{66}^{(l)}V+C_{56}^{(l)}W+e_{16}^{(l)}X+q_{16}^{(l)}Y\right)\\&+l\mathrm{i}kz^{-1}\left(C_{14}^{(l)}U+C_{46}^{(l)}V+C_{45}^{(l)}W+e_{14}^{(l)}X+q_{14}^{(l)}Y\right)\Big]\pi(z)\\&+(\delta(z-0)-\delta(z-h))\left(\frac{z}{h}\right)^l\left(C_{45}^{(l)}U'+C_{44}^{(l)}V'+C_{34}^{(l)}W'+e_{34}^{(l)}X'+q_{34}^{(l)}Y'+\mathrm{i}kC_{14}^{(l)}U\right.\\&\left.+\mathrm{i}kC_{46}^{(l)}V+\mathrm{i}kC_{45}^{(l)}W+\mathrm{i}ke_{14}^{(l)}X+\mathrm{i}kq_{14}^{(l)}Y\right)=-\frac{\rho^{(l)}z^l\omega^2}{h^l}V\pi(z),\end{aligned}\tag{7b}$$

$$\begin{aligned}&\left(\frac{z}{h}\right)^l\Big[C_{35}^{(l)}U''+C_{34}^{(l)}V''+C_{33}^{(l)}W''+e_{33}^{(l)}X''+q_{33}^{(l)}Y''+\mathrm{i}k\left(C_{13}^{(l)}+C_{55}^{(l)}\right)U'\\&+lz^{-1}\left(C_{35}^{(l)}U'+C_{34}^{(l)}V'+C_{33}^{(l)}W'+e_{33}^{(l)}X'+q_{33}^{(l)}Y'\right)+2\mathrm{i}kC_{35}^{(l)}W'+\mathrm{i}k\left(e_{13}^{(l)}+e_{35}^{(l)}\right)X'\\&+\mathrm{i}k\left(q_{13}^{(l)}+q_{35}^{(l)}\right)Y'+\mathrm{i}k\left(C_{36}^{(l)}+C_{45}^{(l)}\right)V'-k^2\left(C_{15}^{(l)}U+C_{56}^{(l)}V+C_{55}^{(l)}W+e_{15}^{(l)}X+q_{15}^{(l)}Y\right)\\&+l\mathrm{i}kz^{-1}\left(C_{13}^{(l)}U+C_{36}^{(l)}V+C_{35}^{(l)}W+e_{13}^{(l)}X+q_{13}^{(l)}Y\right)\Big]\pi(z)\\&+(\delta(z-0)-\delta(z-h))\left(\frac{z}{h}\right)^l\left(C_{35}^{(l)}U'+C_{34}^{(l)}V'+C_{33}^{(l)}W'+e_{33}^{(l)}X'+q_{33}^{(l)}Y'+\mathrm{i}kC_{13}^{(l)}U\right.\\&\left.+\mathrm{i}kC_{36}^{(l)}V+\mathrm{i}kC_{35}^{(l)}W+\mathrm{i}ke_{13}^{(l)}X+\mathrm{i}kq_{13}^{(l)}Y\right)=-\frac{\rho^{(l)}z^l\omega^2}{h^l}W\pi(z),\end{aligned}\tag{7c}$$

$$\begin{aligned}&\left(\frac{z}{h}\right)^l\Big[e_{35}^{(l)}U''+e_{34}^{(l)}V''+e_{33}^{(l)}W''-\varepsilon_{33}^{(l)}X''-g_{33}^{(l)}Y''+\mathrm{i}k\left(e_{15}^{(l)}+e_{31}^{(l)}\right)U'\\&+lz^{-1}\left(e_{35}^{(l)}U'+e_{34}^{(l)}V'+e_{33}^{(l)}W'X'-\varepsilon_{33}^{(l)}-g_{33}^{(l)}\right)+\mathrm{i}k\left(e_{14}^{(l)}+e_{36}^{(l)}\right)V'+\mathrm{i}k\left(e_{13}^{(l)}+e_{35}^{(l)}\right)W'\\&-2\mathrm{i}k\varepsilon_{13}^{(l)}X'-2ikg_{13}^{(l)}Y'-k^2\left(e_{11}^{(l)}U+e_{16}^{(l)}V+e_{15}^{(l)}W-\varepsilon_{11}^{(l)}X-g_{11}^{(l)}Y\right)\\&+l\mathrm{i}kz^{-1}\left(e_{31}^{(l)}U+e_{36}^{(l)}V+e_{35}^{(l)}W-\varepsilon_{13}^{(l)}X-g_{13}^{(l)}Y\right)\Big]\pi(z)\\&+(\delta(z-0)-\delta(z-h))\left(\frac{z}{h}\right)^l\left(e_{35}^{(l)}U'+e_{34}^{(l)}V'+e_{33}^{(l)}W'-\varepsilon_{33}^{(l)}X'-g_{33}^{(l)}Y'+\mathrm{i}ke_{31}^{(l)}U\right.\\&\left.+\mathrm{i}ke_{36}^{(l)}V+\mathrm{i}ke_{35}^{(l)}W-\mathrm{i}k\varepsilon_{13}^{(l)}X-\mathrm{i}kg_{13}^{(l)}Y\right)=0,\end{aligned}\tag{7d}$$

$$
\begin{aligned}
&\left(\frac{z}{h}\right)^l \Big[q_{35}^{(l)}U'' + q_{34}^{(l)}V'' + q_{33}^{(l)}W'' - g_{33}^{(l)}X'' - \mu_{33}^{(l)}Y'' + \mathrm{i}k\left(q_{15}^{(l)} + q_{31}^{(l)}\right)U' \\
&\quad + lz^{-1}\left(q_{35}^{(l)}U' + q_{34}^{(l)}V' + q_{33}^{(l)}W' - g_{33}^{(l)}X' - \mu_{33}^{(l)}Y'\right) + \mathrm{i}k\left(q_{14}^{(l)} + q_{36}^{(l)}\right)V' \\
&\quad - 2\mathrm{i}k\left(g_{13}^{(l)}X' + \mu_{13}^{(l)}Y'\right) - k^2\left(q_{11}^{(l)}U + q_{16}^{(l)}V + q_{15}^{(l)}W - g_{11}^{(l)}X - \mu_{11}^{(l)}Y\right) \\
&\quad + \mathrm{i}k\left(q_{13}^{(l)} + q_{35}^{(l)}\right)W' + l\mathrm{i}kz^{-1}\left(q_{31}^{(l)}U + q_{36}^{(l)}V + q_{35}^{(l)}W - g_{13}^{(l)}X - \mu_{13}^{(l)}Y\right)\Big]\pi(z) \\
&\quad + (\delta(z-0) - \delta(z-h))\left(\frac{z}{h}\right)^l\left(q_{35}^{(l)}U' + q_{34}^{(l)}V' + q_{33}^{(l)}W' - g_{33}^{(l)}X' - \mu_{33}^{(l)}Y' + \mathrm{i}kq_{31}^{(l)}U\right. \\
&\quad \left. + \mathrm{i}kq_{36}^{(l)}V + \mathrm{i}kq_{35}^{(l)}W - \mathrm{i}kg_{13}^{(l)}X - \mathrm{i}k\mu_{13}^{(l)}Y\right) = 0. \qquad (7e)
\end{aligned}
$$

$U(z)$, $V(z)$, $W(z)$, $X(z)$ and $Y(z)$ can be expanded to the Legendre orthogonal polynomial series as follows:

$$
\begin{aligned}
&U(z) = \sum_{m=0}^{\infty} p_m^1 Q_m(z), \quad V(z) = \sum_{m=0}^{\infty} p_m^2 Q_m(z), \quad W(z) = \sum_{m=0}^{\infty} p_m^3 Q_m(z), \\
&X(z) = \sum_{m=0}^{\infty} r_m^1 Q_m(z), \quad Y(z) = \sum_{m=0}^{\infty} r_m^2 Q_m(z), \qquad (8)
\end{aligned}
$$

where $p_m^i (i = 1, 2, 3)$ and $r_m^i (i = 1, 2)$ are the expansion coefficients and

$$
Q_m(z) = \sqrt{\frac{2m+1}{h}} P_m\left(\frac{2z-h}{h}\right)
$$

with P_m being the mth Legendre polynomial. Theoretically, m runs from 0 to ∞. In practice, the summation over the polynomials in Eqs. (8) can be halted at some finite value $m = M$, when higher-order terms become essentially negligible.

Multiplying by $Q_j^*(z)$ with j running from 0 to M, integrating over z from 0 to h, and taking advantage of the orthonormality of the functions $Q_m(z)$, give the following systems:

$$
{}^lA_{11}^{j,m}p_m^1 + {}^lA_{12}^{j,m}p_m^2 + {}^lA_{13}^{j,m}p_m^3 + {}^lA_{14}^{j,m}r_m^1 + {}^lA_{15}^{j,m}r_m^2 = -\omega^2 \cdot {}^lM_m^j p_m^1 \qquad (9a)
$$

$$
{}^lA_{21}^{j,m}p_m^1 + {}^lA_{22}^{j,m}p_m^2 + {}^lA_{23}^{j,m}p_m^3 + {}^lA_{24}^{j,m}r_m^1 + {}^lA_{25}^{j,m}r_m^2 = -\omega^2 \cdot {}^lM_m^j p_m^2 \qquad (9b)
$$

$$
{}^lA_{31}^{j,m}p_m^1 + {}^lA_{32}^{j,m}p_m^2 + {}^lA_{33}^{j,m}p_m^3 + {}^lA_{34}^{j,m}r_m^1 + {}^lA_{35}^{j,m}r_m^2 = -\omega^2 \cdot {}^lM_m^j p_m^3 \qquad (9c)
$$

$$
{}^lA_{41}^{j,m}p_m^1 + {}^lA_{42}^{j,m}p_m^2 + {}^lA_{43}^{j,m}p_m^3 + {}^lA_{44}^{j,m}r_m^1 + {}^lA_{45}^{j,m}r_m^2 = 0 \qquad (9d)
$$

$$
{}^lA_{51}^{j,m}p_m^1 + {}^lA_{52}^{j,m}p_m^2 + {}^lA_{53}^{j,m}p_m^3 + {}^lA_{54}^{j,m}r_m^1 + {}^lA_{55}^{j,m}r_m^2 = 0, \qquad (9e)
$$

where $A_{\alpha\beta}{}^{j,m}(\alpha,\beta = 1,2,3,4)$ and $M_m{}^j$ are the elements of a non-symmetric matrix. They can be obtained according to Eqs. (7).

Eq. (9e) can be written as

$$
r_m^2 = -\left({}^lA_{55}^{j,m}\right)^{-1}\left({}^lA_{51}^{j,m}p_m^1 + {}^lA_{52}^{j,m}p_m^2 + {}^lA_{53}^{j,m}p_m^3 + {}^lA_{54}^{j,m}r_m^1\right). \qquad (10)
$$

Substituting Eq. (10) into Eq. (9d),

$$
\begin{aligned}
r_m^1 = &\left[{}^lA_{45}^{j,m}\left({}^lA_{55}^{j,m}\right)^{-1} \cdot {}^lA_{54}^{j,m} - {}^lA_{44}^{j,m}\right]^{-1}\left\{\left[{}^lA_{41}^{j,m} - {}^lA_{45}^{j,m}\left({}^lA_{55}^{j,m}\right)^{-1} \cdot {}^lA_{51}^{j,m}\right]p_m^1\right. \\
&\left. + \left[{}^lA_{42}^{j,m} - {}^lA_{45}^{j,m}\left({}^lA_{55}^{j,m}\right)^{-1} \cdot {}^lA_{52}^{j,m}\right]p_m^2 + \left[{}^lA_{43}^{j,m} - {}^lA_{45}^{j,m}\left({}^lA_{55}^{j,m}\right)^{-1} \cdot {}^lA_{53}^{j,m}\right]p_m^3\right\}. \qquad (11)
\end{aligned}
$$

Substituting Eq. (11) into Eq. (10),

$$r_m^2 = -\left({}^lA_{55}^{j,m}\right)^{-1}\Big\{{}^lA_{51}^{j,m} + {}^lA_{54}^{j,m}\cdot{}^lIA^{j,m}\Big[\left({}^lA_{41}^{j,m} - {}^lAA^{j,m}\cdot{}^lA_{51}^{j,m}\right)p_m^1 + \left({}^lA_{42}^{j,m} - {}^lAA^{j,m}\cdot{}^lA_{52}^{j,m}\right)p_m^2 + \left({}^lA_{43}^{j,m} - {}^lAA^{j,m}\cdot{}^lA_{53}^{j,m}\right)p_m^3\Big]\Big\}, \quad (12)$$

where

$${}^lAA^{j,m} = {}^lA_{45}^{j,m}\left({}^lA_{55}^{j,m}\right)^{-1}, \quad {}^lIA^{j,m} = \left[{}^lA_{45}^{j,m}\left({}^lA_{55}^{j,m}\right)^{-1}\cdot{}^lA_{54}^{j,m} - {}^lA_{44}^{j,m}\right]^{-1}.$$

Substituting Eqs. (11) and (12) into Eqs. (9a)–(9c),

$$\begin{bmatrix} {}^l\bar{A}_{11}^{j,m} & {}^l\bar{A}_{12}^{j,m} & {}^l\bar{A}_{13}^{j,m} \\ {}^l\bar{A}_{21}^{j,m} & {}^l\bar{A}_{22}^{j,m} & {}^l\bar{A}_{22}^{j,m} \\ {}^l\bar{A}_{31}^{j,m} & {}^l\bar{A}_{32}^{j,m} & {}^l\bar{A}_{33}^{j,m} \end{bmatrix}\begin{Bmatrix} p_m^1 \\ p_m^2 \\ p_m^3 \end{Bmatrix} = -\omega^2\begin{bmatrix} {}^lM_m^j & 0 & 0 \\ 0 & {}^lM_m^j & 0 \\ 0 & 0 & {}^lM_m^j \end{bmatrix}\begin{Bmatrix} p_m^1 \\ p_m^2 \\ p_m^3 \end{Bmatrix}, \quad (13)$$

where

$${}^l\bar{A}_{11}^{j,m} = {}^lA_{11}^{j,m} - {}^lA_{15}^{j,m}\left({}^lA_{55}^{j,m}\right)^{-1}\cdot{}^lA_{51}^{j,m} + \left({}^lA_{14}^{j,m} - {}^lA_{15}^{j,m}\left({}^lA_{55}^{j,m}\right)^{-1}\cdot{}^lA_{54}^{j,m}\right)\cdot{}^lIA^{j,m}\left({}^lA_{41}^{j,m} - {}^lAA^{j,m}\cdot{}^lA_{51}^{j,m}\right),$$

$${}^l\bar{A}_{12}^{j,m} = {}^lA_{12}^{j,m} - {}^lA_{15}^{j,m}\left({}^lA_{55}^{j,m}\right)^{-1}\cdot{}^lA_{52}^{j,m} + \left({}^lA_{14}^{j,m} - {}^lA_{15}^{j,m}\left({}^lA_{55}^{j,m}\right)^{-1}\cdot{}^lA_{54}^{j,m}\right)\cdot{}^lIA^{j,m}\left({}^lA_{42}^{j,m} - {}^lAA^{j,m}\cdot{}^lA_{52}^{j,m}\right),$$

$${}^l\bar{A}_{13}^{j,m} = {}^lA_{13}^{j,m} - {}^lA_{15}^{j,m}\left({}^lA_{55}^{j,m}\right)^{-1}\cdot{}^lA_{53}^{j,m} + \left({}^lA_{14}^{j,m} - {}^lA_{15}^{j,m}\left({}^lA_{55}^{j,m}\right)^{-1}\cdot{}^lA_{54}^{j,m}\right)\cdot{}^lIA^{j,m}\left({}^lA_{43}^{j,m} - {}^lAA^{j,m}\cdot{}^lA_{53}^{j,m}\right),$$

$${}^l\bar{A}_{21}^{j,m} = {}^lA_{21}^{j,m} - {}^lA_{25}^{j,m}\left({}^lA_{55}^{j,m}\right)^{-1}\cdot{}^lA_{51}^{j,m} + \left({}^lA_{24}^{j,m} - {}^lA_{25}^{j,m}\left({}^lA_{55}^{j,m}\right)^{-1}\cdot{}^lA_{54}^{j,m}\right)\cdot{}^lIA^{j,m}\left({}^lA_{41}^{j,m} - {}^lAA^{j,m}\cdot{}^lA_{51}^{j,m}\right),$$

$${}^l\bar{A}_{22}^{j,m} = {}^lA_{22}^{j,m} - {}^lA_{25}^{j,m}\left({}^lA_{55}^{j,m}\right)^{-1}\cdot{}^lA_{52}^{j,m} + \left({}^lA_{24}^{j,m} - {}^lA_{25}^{j,m}\left({}^lA_{55}^{j,m}\right)^{-1}\cdot{}^lA_{54}^{j,m}\right)\cdot{}^lIA^{j,m}\left({}^lA_{42}^{j,m} - {}^lAA^{j,m}\cdot{}^lA_{52}^{j,m}\right),$$

$${}^l\bar{A}_{23}^{j,m} = {}^lA_{23}^{j,m} - {}^lA_{25}^{j,m}\left({}^lA_{55}^{j,m}\right)^{-1}\cdot{}^lA_{53}^{j,m} + \left({}^lA_{24}^{j,m} - {}^lA_{25}^{j,m}\left({}^lA_{55}^{j,m}\right)^{-1}\cdot{}^lA_{54}^{j,m}\right)\cdot{}^lIA^{j,m}\left({}^lA_{43}^{j,m} - {}^lAA^{j,m}\cdot{}^lA_{53}^{j,m}\right),$$

$$
\begin{aligned}
{}^{l}\bar{A}_{31}^{j,m} &= {}^{l}A_{31}^{j,m} - {}^{l}A_{35}^{j,m}\left({}^{l}A_{55}^{j,m}\right)^{-1}\cdot{}^{l}A_{51}^{j,m} \\
&\quad + \left({}^{l}A_{34}^{j,m} - {}^{l}A_{35}^{j,m}\left({}^{l}A_{55}^{j,m}\right)^{-1}\cdot{}^{l}A_{54}^{j,m}\right)\cdot{}^{l}IA^{j,m}\left({}^{l}A_{41}^{j,m} - {}^{l}AA^{j,m}\cdot{}^{l}A_{51}^{j,m}\right),
\end{aligned}
$$

$$
\begin{aligned}
{}^{l}\bar{A}_{32}^{j,m} &= {}^{l}A_{32}^{j,m} - {}^{l}A_{35}^{j,m}\left({}^{l}A_{55}^{j,m}\right)^{-1}\cdot{}^{l}A_{52}^{j,m} \\
&\quad + \left({}^{l}A_{34}^{j,m} - {}^{l}A_{35}^{j,m}\left({}^{l}A_{55}^{j,m}\right)^{-1}\cdot{}^{l}A_{54}^{j,m}\right)\cdot{}^{l}IA^{j,m}\left({}^{l}A_{42}^{j,m} - {}^{l}AA^{j,m}\cdot{}^{l}A_{52}^{j,m}\right),
\end{aligned}
$$

$$
\begin{aligned}
{}^{l}\bar{A}_{33}^{j,m} &= {}^{l}A_{33}^{j,m} - {}^{l}A_{35}^{j,m}\left({}^{l}A_{55}^{j,m}\right)^{-1}\cdot{}^{l}A_{53}^{j,m} \\
&\quad + \left({}^{l}A_{34}^{j,m} - {}^{l}A_{35}^{j,m}\left({}^{l}A_{55}^{j,m}\right)^{-1}\cdot{}^{l}A_{54}^{j,m}\right)\cdot{}^{l}IA^{j,m}\left({}^{l}A_{43}^{j,m} - {}^{l}AA^{j,m}\cdot{}^{l}A_{53}^{j,m}\right).
\end{aligned}
$$

Hence, Eqs. (13) yield a form of the eigenvalue problem. The eigenvalue ω^2 gives the angular frequency of the guided wave; eigenvectors $p_m^i (i = 1, 2, 3)$ allows the components of the particle displacement to be calculated; ${r_m}^1$ and ${r_m}^2$, which can be got according to Eqs. (11) and (12), determined the electric potential and magnetic potential distributions. According to $Vph = \omega/k$ and $Vg = \mathrm{d}\omega/\mathrm{d}k$, the phase velocity and group velocity can be obtained. The complex matrix equations (13) can be solved numerically making use of standard computer programs for the diagonalization of non-symmetric square matrices. In practice, the summation over the polynomials in the $3(M+1)$ eigenmode are generated from the order M of the expansion. Acceptable solutions are those eigenmode for which convergence is obtained as M is increased. We determine that the eigenvalues obtained are converged solutions when a further increase in the matrix dimension does not result in a significant change in the eigenvalue. The computer program was written using Mathmatica.

When the material is orthotropic or has fewer independent constants in the wave propagation direction, and is polarized in the thickness direction, the governing differential equations are reduced to

$$
\begin{aligned}
&\left(\frac{z}{h}\right)^{l}\Big[C_{55}^{(l)}U'' + lz^{-1}C_{55}^{(l)}U' + \mathrm{i}k\left(C_{13}^{(l)} + C_{55}^{(l)}\right)W' + \mathrm{i}k\left(e_{15}^{(l)} + e_{31}^{(l)}\right)X' + \mathrm{i}k\left(q_{15}^{(l)} + q_{31}^{(l)}\right)Y' \\
&\quad - k^2 C_{11}^{(l)}U + l\mathrm{i}kz^{-1}\left(C_{55}^{(l)}W + e_{15}^{(l)}X + q_{15}^{(l)}Y\right)\Big]\pi(z) + (\delta(z-0) - \delta(z-h))\left(\frac{z}{h}\right)^{l}\Big(C_{55}^{(l)}U' \\
&\quad + \mathrm{i}kC_{55}^{(l)}W + \mathrm{i}ke_{15}^{(l)}X + \mathrm{i}kq_{15}^{(l)}Y\Big) = -\frac{\rho^{(l)}z^{l}\omega^2}{h^l}U\pi(z),
\end{aligned}
\tag{14a}
$$

$$
\left(\frac{z}{h}\right)^{l}\Big[C_{44}^{(l)}V'' + lz^{-1}C_{44}^{(l)}V' - k^2C_{66}^{(l)}V\Big]\pi(z) + (\delta(z-0) - \delta(z-h))\left(\frac{z}{h}\right)^{l}C_{44}^{(l)}V' = -\frac{\rho^{(l)}z^{l}\omega^2}{h^l}V\pi(z),
\tag{14b}
$$

$$
\begin{aligned}
&\left(\frac{z}{h}\right)^{l}\Big[C_{33}^{(l)}W'' + e_{33}^{(l)}X'' + q_{33}^{(l)}Y'' + \mathrm{i}k\left(C_{13}^{(l)} + C_{55}^{(l)}\right)U' + lz^{-1}\left(C_{33}^{(l)}W' + e_{33}^{(l)}X' + q_{33}^{(l)}Y'\right) \\
&\quad + l\mathrm{i}kz^{-1}C_{13}^{(l)}U - k^2\left(C_{55}^{(l)}W + e_{15}^{(l)}X + q_{15}^{(l)}Y\right)\Big]\pi(z) + (\delta(z-0) - \delta(z-h))\left(\frac{z}{h}\right)^{l}\Big(C_{33}^{(l)}W' \\
&\quad + e_{33}^{(l)}X' + q_{33}^{(l)}Y' + \mathrm{i}kC_{13}^{(l)}U + \mathrm{i}ke_{13}^{(l)}X + \mathrm{i}kq_{13}^{(l)}Y\Big) = -\frac{\rho^{(l)}z^{l}\omega^2}{h^l}W\pi(z),
\end{aligned}
\tag{14c}
$$

$$
\begin{aligned}
&\left(\frac{z}{h}\right)^{l}\Big[e_{33}^{(l)}W'' - \varepsilon_{33}^{(l)}X'' - g_{33}^{(l)}Y'' + \mathrm{i}k\left(e_{15}^{(l)} + e_{31}^{(l)}\right)U' + lz^{-1}\left(e_{33}^{(l)}W' - \varepsilon_{33}^{(l)}X' - g_{33}^{(l)}Y'\right) \\
&\quad + l\mathrm{i}kz^{-1}e_{31}^{(l)}U - k^2e_{15}^{(l)}W + k^2\varepsilon_{11}^{(l)}X + k^2g_{11}^{(l)}Y\Big]\pi(z) \\
&\quad + (\delta(z-0) - \delta(z-h))\left(\frac{z}{h}\right)^{l}\Big(e_{33}^{(l)}W' - \varepsilon_{33}^{(l)}X' - g_{33}^{(l)}Y' + \mathrm{i}ke_{31}^{(l)}U\Big) = 0,
\end{aligned}
\tag{14d}
$$

Table 1
The material properties of the two materials with polarization in the thickness direction [17]

Property	C_{11}	C_{12}	C_{13}	C_{22}	C_{23}	C_{33}	C_{44}	C_{55}	C_{66}
Ba_2TiO_3	166	77	78	166	78	162	43	43	44.6
$CoFe_2O_4$	286	173	170.5	286	170.5	269.5	45.3	45.3	56.5
	e_{15}	e_{24}	e_{31}	e_{32}	e_{33}	ϵ_{11}	ϵ_{22}	ϵ_{33}	ρ
Ba_2TiO_3	11.6	11.6	−4.4	−4.4	18.6	112	112	126	5.8
$CoFe_2O_4$	0	0	0	0	0	0.8	0.8	0.93	5.3
	q_{15}	q_{24}	q_{31}	q_{32}	q_{33}	μ_{11}	μ_{22}	μ_{33}	
Ba_2TiO_3	0	0	0	0	0	5	5	10	
$CoFe_2O_4$	550	550	580.3	580.3	699.7	−590	−590	157	

Units: C_{ij} ($10^9\,N/m^2$), ϵ_{ij} ($10^{-10}\,F/m^2$), e_{ij} (C/m), q_{ij} (N/Am), μ_{ij} ($10^{-6}\,Ns^2/C^2$), ρ ($10^3\,kg/m^3$).

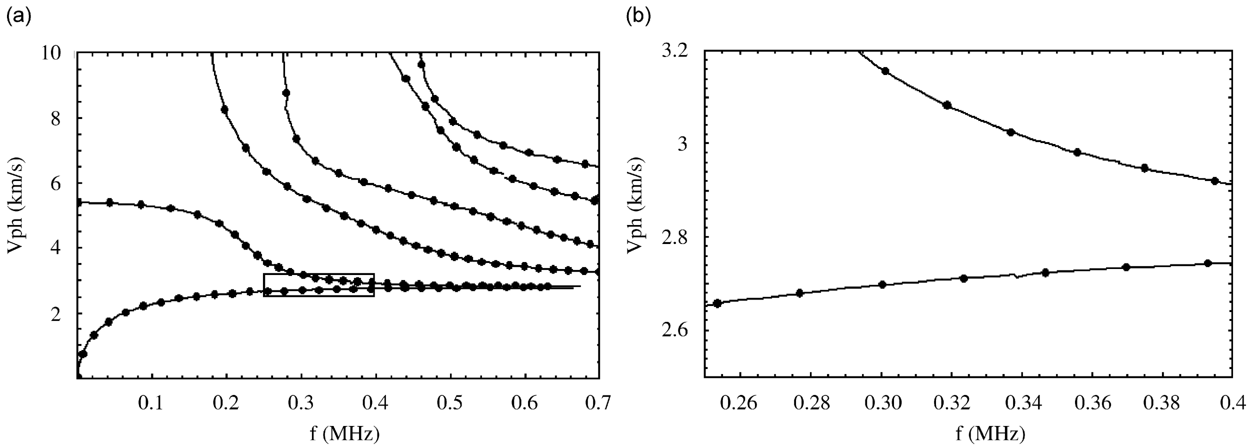

Fig. 1. Phase velocity spectra for the Ba_2TiO_3–$CoFe_2O_4$ FGM plate: dotted line, with magneto-electric coefficients; solid line, without magneto-electric coefficients.

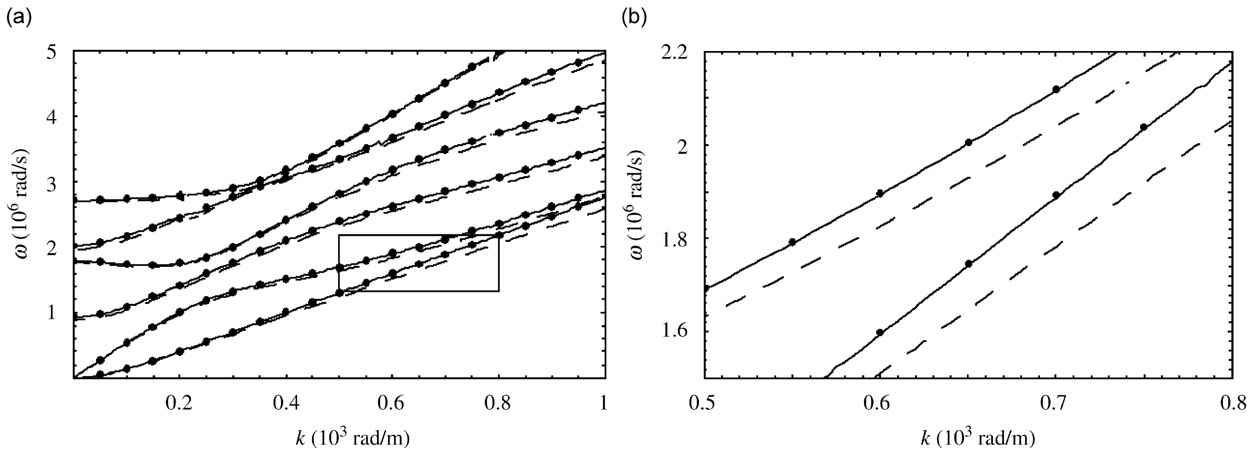

Fig. 2. Frequency spectra for FGM plate: solid line, piezoelectric–piezomagnetic composite plate; dotted line, piezoelectric plate; dashed line, piezomagnetic plate.

$$\left(\frac{z}{h}\right)^{l}\Big[q_{33}^{(l)}W'' - g_{33}^{(l)}X'' - \mu_{33}^{(l)}Y'' + \mathrm{i}k\left(q_{15}^{(l)} + q_{31}^{(l)}\right)U' + l\mathrm{i}kz^{-1}q_{31}^{(l)}U$$
$$+ lz^{-1}\left(q_{33}^{(l)}W' - g_{33}^{(l)}X' - \mu_{33}^{(l)}Y'\right) - k^2q_{15}^{(l)}W + k^2g_{11}^{(l)}X + k^2\mu_{11}^{(l)}Y\Big]\pi(z)$$
$$+ (\delta(z-0) - \delta(z-h))\left(\frac{z}{h}\right)^{l}\left(q_{33}^{(l)}W' - g_{33}^{(l)}X' - \mu_{33}^{(l)}Y' + \mathrm{i}kq_{31}^{(l)}U\right) = 0. \quad (14e)$$

Here, Eq. (14b) is independent of the other four equations. In fact, Eq. (14b) represents the propagating SH wave. It is not influenced by the electric field and magnetic field when the material is polarized in the thickness direction. Eqs. (14a) and (14c) control the propagating Lamb-like wave and are coupled with the electric field and magnetic field.

3. Numerical results

Because the effective modulli of the piezoelectric–piezomagnetic composite is not yet the last word, the Voigt-type model is used here to calculate the effective modulli (except for the magneto–electric coefficients) of two combined piezoelectric–piezomagnetic materials. It is expressed as

$$P(z) = P_1V_1(z) + P_2V_2(z) \quad (15)$$

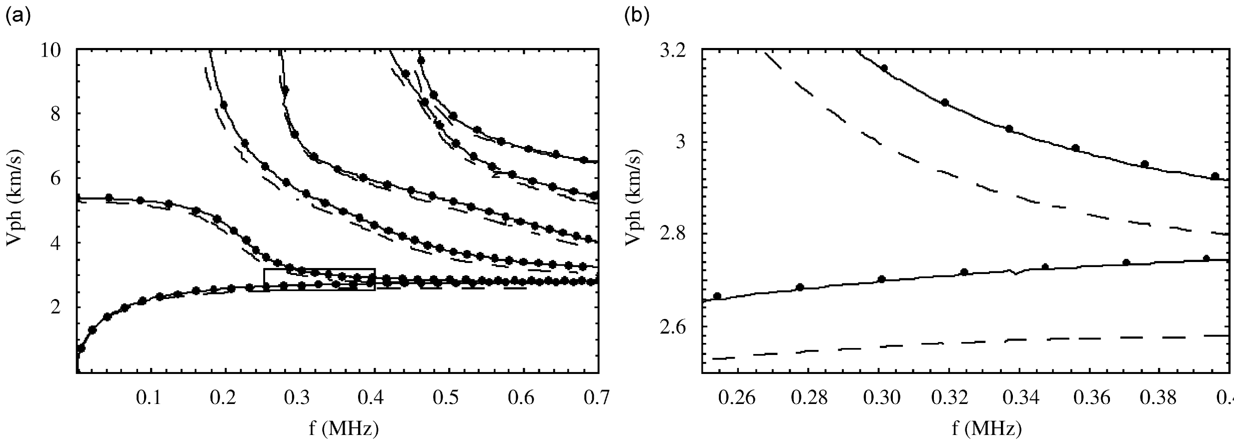

Fig. 3. Phase velocity spectra for FGM plate: solid line, piezoelectric–piezomagnetic composite plate; dotted line, piezoelectric plate; dashed line, piezomagnetic plate.

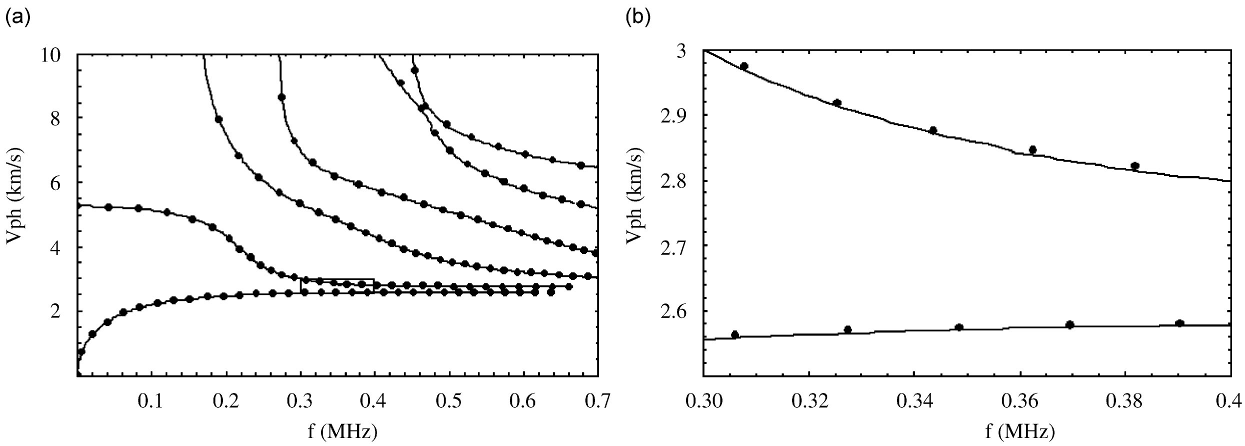

Fig. 4. Phase velocity spectra for FGM plate: solid line, piezomagnetic plate; dotted line, elastic plate.

where $V_i(z)$ and P_i, respectively, denote the volume fraction of the ith material and the corresponding property of the ith material. Here, $\sum V_i(z) = 1$. Hence, the properties of the graded material can be expressed as

$$P(z) = P_2 + (P_1 - P_2)V_1(z). \tag{16}$$

According to Eq. (4), the gradient field of the material volume fraction can be expressed as a power series expansion. The coefficients of the power series can be determined using the Mathematica function 'Fit'.

Based on the foregoing formulations, a computer program has been written to calculate the dispersion curves for the FGM magneto-electro-elastic plate composed of piezoelectric $BaTiO_3$ (bottom) and magnetostrictive $CoFe_2O_4$ (top) with thickness $h = 10$ mm. Their material constants are listed in Table 1 with thickness polarization and the other constants all being zero except for the magneto–electric coefficients. The model of the multiphase method from Li and Dunn [17] is used to calcullate the magneto–electric coefficients. The series expansion equations (8) are truncated at $M = 10$ for all the undermentioned calculations. The gradient field used here is $C(z) = C_B + (C_C - C_B)z/h$.

The Lamb-like wave phase velocity dispersion curves for the FGM piezoelectric–piezomagnetic plate are shown in Fig. 1, in which the solid lines are the dispersion curves without considering the magneto-electric coefficients. Fig. 1(b) is the enlarged figure of the pane in Fig. 1(a). It can be seen that the magneto-electric coefficients have little influence on the dispersion curves. So, the values of the magneto-electric coefficients are unchanged in the undermentioned examples.

Figs. 2 and 3 are the Lamb-like wave frequency spectra and phase velocity spectra for the FGM piezoelectric–piezomagnetic plate and the corresponding non-piezoelectric, non-piezomagnetic plates. Figs. 2(b) and 3(b) are the enlarged figures of the panes in Figs. 2(a) and 3(a). Obviously, the curves of the piezoelectric–piezomagnetic plate and those of the piezoelectric plate are very close to each other, but those of the piezomagnetic plate are much below them. So, it can be assumed that the piezomagnetic effect is much weaker than the piezoelectric effect on the dispersion curves of the Ba_2TiO_3–$CoFe_2O_4$ FGM plate. In order to further approve this viewpoint, Fig. 4 gives the phase velocity spectra for the FGM piezomagnetic plate and the corresponding FGM elastic plate. The two dispersion curves are also very close. The velocity of the piezomagnetic plate is a little above the elastic plate.

Figs. 5 and 6 are the electric potential and magnetic potential distributions of the Ba_2TiO_3–$CoFe_2O_4$ FGM plate at $k = 100$ and 30000 rad/m. In spite of the wavenumber, the amplitudes of the electric potential are far

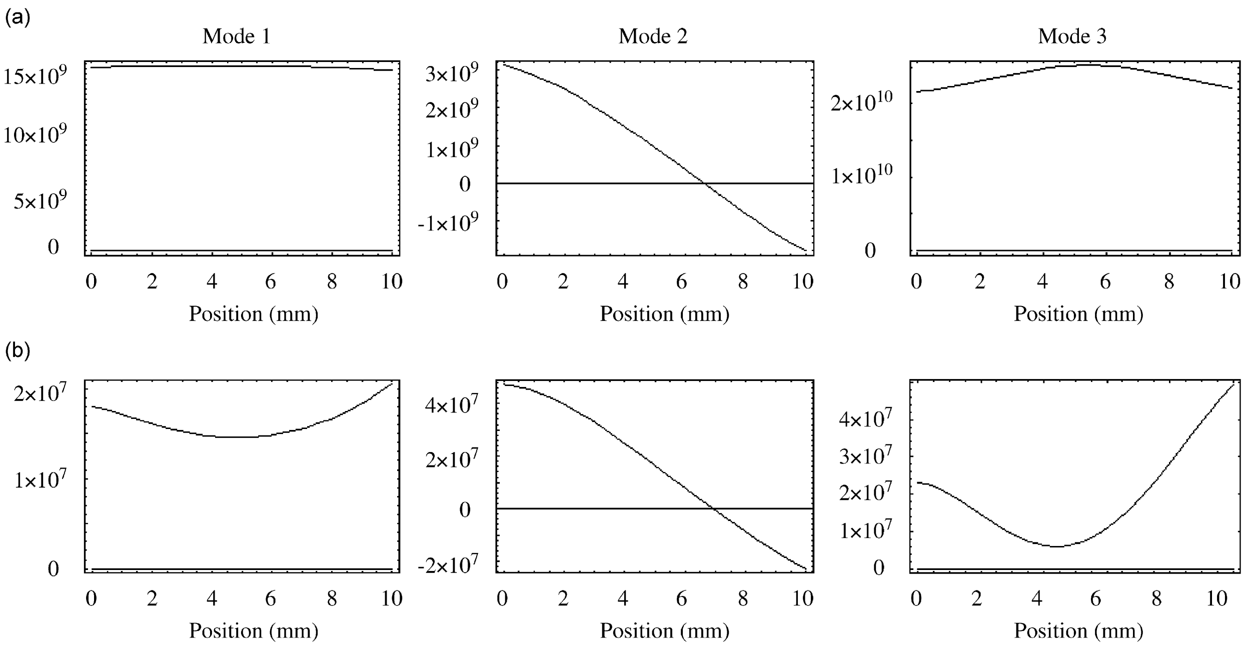

Fig. 5. Potential distributions of the Ba_2TiO_3–$CoFe_2O_4$ FGM plate at $k = 100$ rad/m: (a) electric potential and (b) magnetic potential.

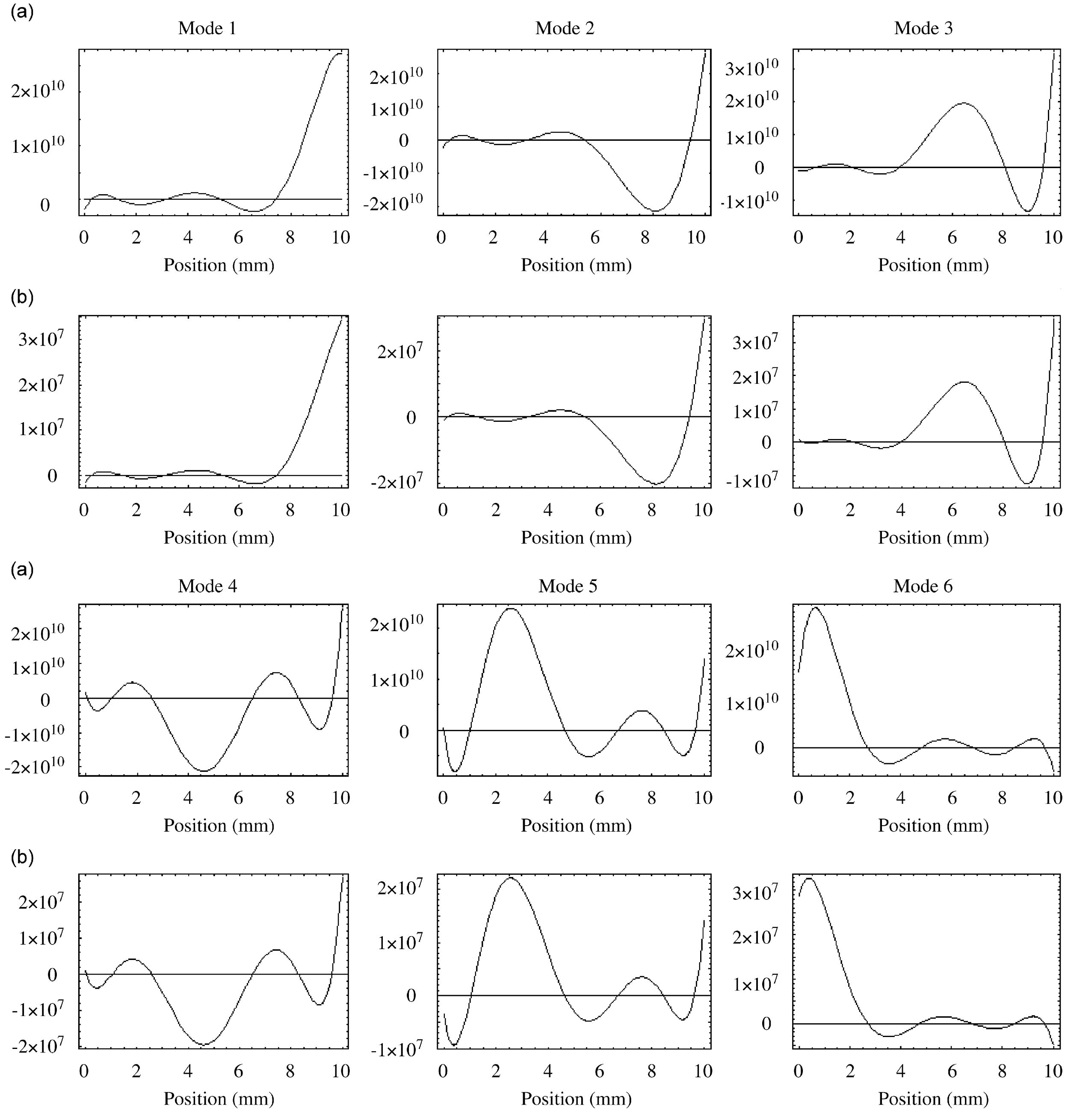

Fig. 6. Potential distributions of the Ba_2TiO_3–$CoFe_2O_4$ FGM plate at $k = 30\,000$ rad/m: (a) electric potential and (b) magnetic potential.

greater than those of the magnetic potential. Not considering the amplitudes, the trends of the electric potential and magnetic potential are similar for the large wavenumber, but are very different for the small wavenumber. Furthermore, for the large wavenumber, the electric potential and magnetic potential distribute mostly near the two surfaces and distribute mostly near the top for the lowest three modes.

The phenomenon that the piezoelectric effect is stronger than the piezomagnetic effect can be explained by Eq. (13) and Table 1. From Eq. (13) we can see that the influential factors of the piezoelectricity and piezomagnetism are similar. The influences are directly proportional to the piezoelectric and piezomagnetic constants and are in inverse ratio to the dielectric and magnetic permeability coefficients. From Table 1, it can be seen that the average piezomagnetic constant is about 50 times of the average piezoelectric constant, but the average magnetic permeability coefficient is about 5000 times of the average dielectric coefficient. As is well known, the velocity in the piezoelectric material is above the velocity in the corresponding non-piezoelectric material. But in this example, the velocity in the piezomagnetic material is a little below the velocity in the corresponding non-piezomagnetic material, which is because the two larger magnetic permeability coefficients in $CoFe_2O_4$ is negative.

In order to validate the judgement, the magnetic permeability coefficients in Table 1 are reduced 100 times and then are taken as absolute values. Fig. 7 is the frequency spectra and phase velocity spectra for the plate of the changed magnetic permeability coefficients. In this case, the piezomagnetic effect is considerable, and even exceeds the piezoelectric effect in some modes. Moreover, the piezomagnetic effect dos not make the dispersion curves move downwards but move upwards.

Another point in Fig. 7 should be paid attention to. At some frequencies, piezomagnetic effect is more considerable than piezoelectric effect, but at some other frequencies the case is quite the contrary. In order to elaborate the different effect of the piezoelectricity and piezomagnetism on the dispersion curves, another example is considered. In this example, we take the values of the piezomagnetic and magnetic permeability coefficients of the $CoFe_2O_4$ to be equal to the piezoelectric and dielectric coefficients of Ba_2TiO_3, respectively; the magnetic permeability coefficients of Ba_2TiO_3, and the dielectric coefficients of $CoFe_2O_4$ are zeroes; and other constants keep unchanged. Fig. 8 is the frequency spectra for this plate. It can be seen that when the wavenumber is small, the dispersion curves for the piezoelectric plate and the piezomagnetic plate is of superposition, i.e. the piezomagnetic effect and piezoelectric effect are equal. However, as the wavenumber increases, the two curves deviate from each other. The piezoelectric effect becomes stronger than the piezomagnetic effect for the first mode; but for the second mode, the piezomagnetic effect becomes stronger.

4. Conclusions

Using the Legendre orthogonal polynomial series expansion method, the wave characteristics in the FGM piezoelectric–piezomagnetic plates are discussed. Based on the calculated results, the following conclusions can be drawn:

(a) When the plate is orthotropic and is polarized in the thickness direction, the independent SH wave is not influenced by the electric field and magnetic field.
(b) In the Ba_2TiO_3–$CoFe_2O_4$ FGM plate, the magneto-electric coefficients have little influence on the dispersion curves.

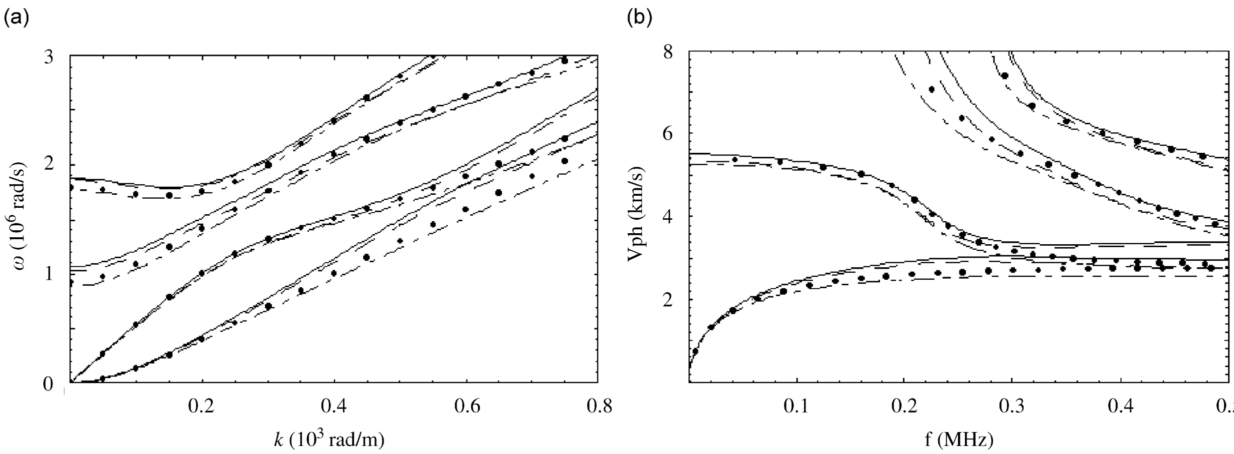

Fig. 7. Dispersion curves for FGM plate with the changed magnetic permeability coefficients: solid line, piezoelectric–piezomagnetic composite plate; dotted line, piezoelectric plate; dashed line, piezomagnetic plate; point curve transformation, elastic plate; (a) frequency spectra and (b) phase velocity spectra.

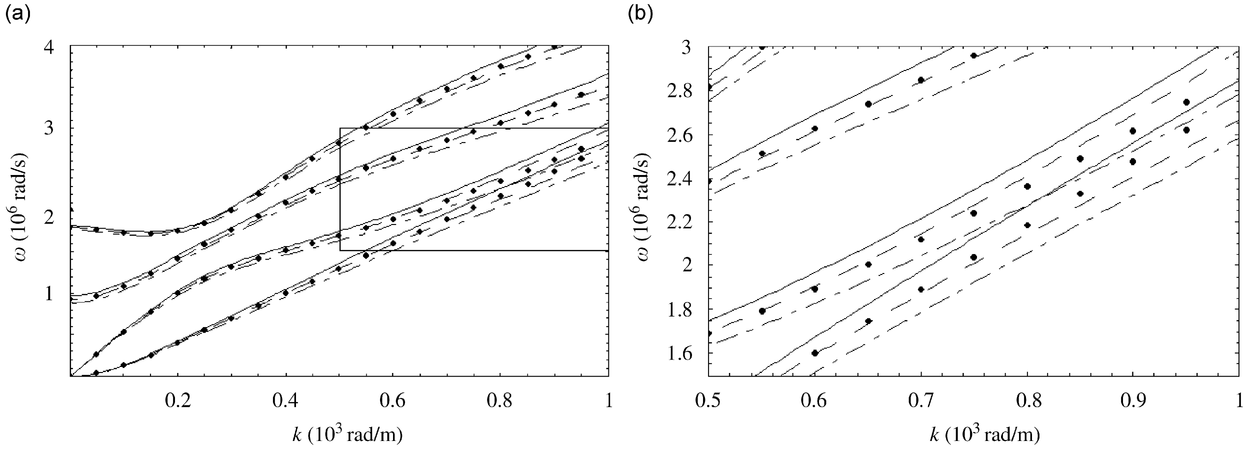

Fig. 8. Frequency spectra for the FGM piezoelectric–piezomagnetic plate with equal magneto and electric constants: solid line, piezoelectric–piezomagnetic composite plate; dotted line, piezoelectric plate; dashed line, piezomagnetic plate; point curve transformation, elastic plate.

(c) The influential factors of the piezoelectricity and piezomagnetism on the wave characteristics are similar. The influences are directly proportional to the piezoelectric and piezomagnetic constants and are inversely proportional to the dielectric and magnetic permeability coefficients. In the Ba_2TiO_3–$CoFe_2O_4$ FGM plate, the piezoelectric effect is far stronger than the piezomagnetic effect.
(d) For different Lamb-like wave modes, the piezoelectric effect is different from the piezomagnetic effect.
(e) The trends of the electric potential and magnetic potential are similar for large wavenumbers, but are very different for small wavenumbers. Moreover, the electric potential and magnetic potential distribute mostly near the surface for large wavenumbers.

References

[1] J.D. Achenbach, Quantitative nondestructive evaluation, *International Journal of Solids and Structures* 37 (2000) 13–27.
[2] G.R. Buchanan, Comparison of effective moduli for multiphase magneto-electro-elastic materials, *Proceedings of the Tenth International Conference on Composite/Nano Engineering*, New Orleans, 2003.
[3] E. Pan, Exact solution for simply supported and multilayered magneto-electro-elastic plates, *Journal of Applied Mechanics* 68 (2001) 608–618.
[4] E. Pan, P.R. Heyliger, Free vibrations of simply supported and multilayered magneto-electro-elastic plates, *Journal of Sound and Vibration* 252 (2002) 429–442.
[5] W.Q. Chen, Kang Yong Lee, H.J. Ding, On free vibration of non-homogeneous transversely isotropic magneto-electro-elastic plates, *Journal of Sound and Vibration* 279 (2005) 237–251.
[6] X. Wang, Y.P. Shen, The general solution of three-dimensional problems in magneto-electro-elastic media, *International Journal of Engineering Science* 40 (2002) 1069–1080.
[7] X. Wang, Y.P. Shen, Inclusions of arbitrary shape in magneto-electro-elastic composite materials, *International Journal of Engineering Science* 41 (2003) 85–102.
[8] P.F. Hou, A.Y.T. Leung, The transient response of magneto-electro-elastic hollow cylinders, *Smart Material Structure* 13 (2004) 762–776.
[9] W.Q. Chen, Kang Yong Lee, H.J. Ding, General solution for transversely isotropic magneto-electro-thermo-elasticity and the potential theory method, *International Journal of Engineering Science* 42 (2004) 1361–1379.
[10] P.F. Hou, H.J. Ding, A.Y.T. Leung, The transient responses of a special non-homogeneous magneto-electro-elastic hollow cylinder for axisymmetric plane strain problem, *Journal of Sound and Vibration* 291 (2006) 19–47.
[11] P. Chen, Y. Shen, Propagation of axial shear magneto-electro-elastic waves in piezoelectric–piezomagnetic composites with randomly distributed cylindrical inhomogeneities, *International Journal of Solids and Structures* 44 (2007) 1511–1532.
[12] J. Wei, X.Y. Su, Wave propagation and energy transportation along cylindrical piezoelectric piezomagnetic material, *AcLa ScienLiarum NaLuralium LniversiLaLis Pekinensis* 42 (2006) 310–314 (in Chinese).

[13] J.Y. Chen, H.L. Chen, Love wave propagation in magneto-electro-elastic multilayered structures, *Acta Materiae Compositae Sinica* 23 (2006) 181–184 (in Chinese).
[14] J.Y. Chen, E. Pan, H.L. Chen, Wave propagation in magneto-electro-elastic multilayered plates, *International Journal of Solids and Structures* 44 (2007) 1073–1085.
[15] J.E. Lefebvre, V. Zhang, J. Gazalet, T. Gryba, Legendre polynomial approach for modeling free-ultrasonic waves in multilayered plates, *Journal of Applied Physics* 85 (1999) 3419–3427.
[16] J.E. Lefebvre, V. Zhang, J. Gazalet, T. Gryba, Acoustic wave propagation in continuous functionally graded plates, an extension of the Legendre polynomial approach, *IEEE Transactions on Ultrasonics, Ferroelectrics and Frequency Control* 48 (2001) 1332–1340.
[17] J.Y. Li, M.L. Dunn, Micromechanics of magnetoelectroelastic composite materials average field and effective behavior, *Journal of Intelligent Material Systems and Structures* 9 (1998) 404–416.